PROCEEDINGS OF SCIENCE

Effects of bias voltage during priming on operation of diamond detectors *

Gregor Kramberger[†a], **V. Cindro**[a], **A. Gorišek**[a], **I. Mandić**[a], **M. Mikuž**[a,b], **M. Zavrtanik**[a] ‡

[a] *Jozef Stefan Institute*

[b] *University of Ljubljana, Faculty of Mathematics and Physics, Department of Physics*

E-mail: Gregor.Kramberger@ijs.si

Effects of bias voltage during priming of single crystalline diamond detectors were investigated with the Transient Current Technique. Already after irradiation to relatively low fluence of $1.1 \cdot 10^{14}$ reactor neutrons/cm^2 the electric field profiles differ very much regarding to the biasing conditions. A novel method was presented for the determination of space charge from charge collection measurements for ^{90}Sr electrons. It was used for investigation of poly crystalline detectors where significant space charge is present already before irradiation.

21st *International Workshop on Vertex Detectors*
September 16-21 2012
Jeju Island, Republic of Korea

*Work performed in the framework of CERN-RD42 collaboration.

†Speaker.

‡G. Kramberger, V. Cindro, A. Gorivšek, I. Mandić, M. Mikuž and M. Zavrtanik are with the Jožef Stefan Institute, Jamova 39, SI-1000 Ljubljana, Slovenia (Tel: (+386) 1 4773512, fax: (+386) 1 4773166,), M. Mikuž is also with University of Ljubljana, Faculty of Mathematics and Physics, Department of Physics, Jadranska 19, SI-1000 Ljubljana.

PoS(Vertex 2012)013

1. Introduction

Diamond detectors are the most serious contenders to silicon detectors for use in future high energy physics experiments. The main obstacles for employing any semiconductor sensor technology for tracking and vertexing at future experiments are often radiation damage effects. At the upgraded Large Hadron Collider the most exposed sensors will face $> 10^{16}$ hadrons/cm^2 [1]. Diamond has many advantages over silicon such as lower capacitance (i.e. smaller noise), fast response, very low leakage current (wide band-gap E_g), excellent thermal conductivity, but it suffers from the larger ionization energy which results in lower signal [2]. On average 36 e-h pairs/μm are created by a minimum ionizing particle.

Diamond detectors are mainly grown with the Chemical Vapour Deposition (CVD) technique. There are two flavours of detectors regarding the substrate used for growth. The single crystal detector (scCVD) is grown on a high-pressure high-temperature diamond substrate and forms a perfect diamond lattice. On the other hand, poly crystalline detector (pCVD) is grown on a non-diamond substrate, therefore small crystal grains in random orientations start forming on the substrate. The grains grow, and the larger ones have the tendency to grow faster, terminating the growth of the smaller ones. Therefore the average grain size increases across the pCVD thickness from the substrate to the growth side.

Imperfections in the crystal result in trapping centres and the drifting charge is trapped in pCVD already before irradiation. The charge collection distance (*CCD*) is therefore often used to characterize the material. *CCD* corresponds to the average distance the electron-hole pairs move apart. In thin diamond *CCD* is limited by the sensor dimension, while in thick (thickness $\gg$ *CCD*) diamond *CCD* approaches the sum of mean free paths of electrons and holes. There is very little trapping in scCVD, and therefore its *CCD* matches the detector thickness. State of the art pCVD detectors have $CCD \approx 200 - 300$ μm at electric field of 2 V/μm [3] which corresponds to signal between 7000-9000 electrons.

Impinging particles displace the carbon atoms from their lattice sites and give rise to energy levels in the band-gap which behave as traps. In contrast to silicon, radiation induced levels exhibit no noticeable effect on the leakage current, as even if located close to mid-gap ($E_t \sim 2.5$ eV) they can't act as generation centres at room temperature. They can, however, trap drifting charge. If sufficiently separated from the conduction/valence band (deep traps) the de-trapping times are large, even of order of months, so the charge is lost for the signal. Usually an occupied trap cannot trap the same charge carrier, so it remains passivized for the de-trapping time. It can, however, trap the carrier of the opposite charge, effectively serving as a recombination centre. The cross sections for the capture of the two carrier species (electrons and holes) can differ by orders of magnitude, with the larger cross section exhibited by a charged trap than the neutral one. This forms the fundamental principle of the priming ("pumping") procedure, where diamonds are exposed to ionizing radiation, which fills the traps and passivates them. Priming is done before the measurement using a strong ^{90}Sr source. It is inherently present in hadron colliders where tracking detectors are exposed to charged particle fluxes in excess of MHz/cm^2.

Almost all measurements of *CCD* in the past were made after priming the detector without the bias voltage applied. The priming was followed by measurements in test beam or in the lab, in both cases usually at much smaller particle rates, far from those at LHC experiments. Under the bias the

carriers move and charge trapped at the energy levels in the band gap alters the space charge and hence the electric field in the detector. Different carrier species drift to opposing electrodes, hence space charge of opposite polarity is present at both ends of the detector. This process is usually called polarization.

The consequence of the large band-gap are long de-trapping times, hence even traps with capture cross-section orders of magnitude smaller than the dominant ones can contribute to the space charge. A steady state of space charge distribution can therefore be reached on the time scale of hours/days depending on particle rates and bias voltage. The aim of this work is to show the impact of applied bias voltage on internal electric field during priming. Transient current technique is an ideal tool to study it on scCVD, while for pCVD a novel approach of probing the field from charge collection efficiency measurements will be introduced.

2. Samples and experimental techniques

Two pad detectors, one scCVD and one pCVD were selected for the studies. Geometrically they were identical, 4x4 mm^2 wide with a circular metalization (diameter=2 mm) on both sides of the diamond. It was done by Ohio State University [4] using their proprietary process. The samples were 500 μm thick. The *CCD* for the pCVD diamond was 240 μm. For this study only the scCVD detector was irradiated, by neutrons, to relatively low fluence of $\Phi = 1.1 \cdot 10^{14}$ fast neutrons/cm^2 (> 100 keV) at the Jozef Stefan Institute research reactor [5]. After the irradiation the detector was kept at room temperature for a period of months during which different measurements took place.

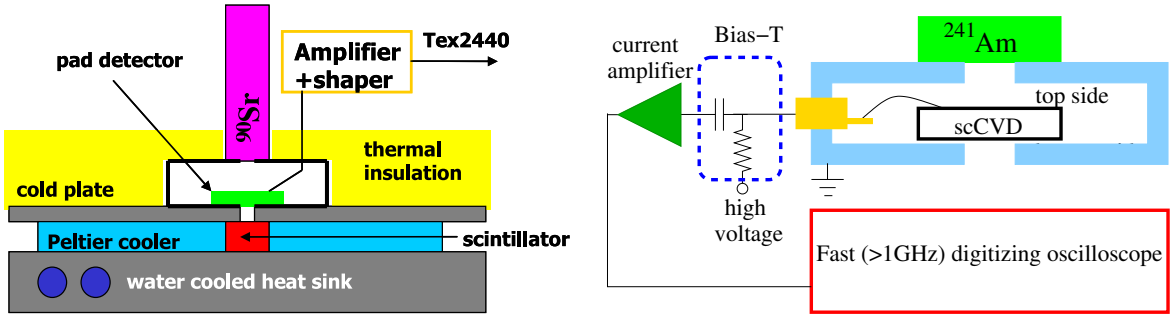

(a) (b)

Figure 1: Schematic view of the experimental setup: (a) for charge collection measurements with ^{90}Sr electrons and (b) for Transient Current Technique using α particles. The bias polarity is referenced to bias applied to the top of the detector with back detector at chassis ground.

Both detectors were mounted in aluminium housing which had openings at both sides allowing exposure to alpha particles from an ^{241}Am and electrons from a 37 MBq ^{90}Sr source. The setup shown in Fig. 1a was used for measurement of the signal of ^{90}Sr electrons. The openings in thick aluminium served as collimators for the electrons. Thus, in $> 97\%$ of events triggered by the scintillator coupled to the photo-multiplier, the electron crossed the detector, which enabled measurements also at low signal-to-noise ratios. The induced current is fed in the preamplifier followed by a 500 ns shaping amplifier. The pulses are recorded by a digital oscilloscope. More details about the setup and analysis can be found in [6].

The setup schematically shown in Fig.1b was used for measuring transient currents after exposure to alpha particles. Their penetration depth in diamond is of order 10 μm. Carriers of one type are immediately swept to the neighbouring electrode while carriers of the opposite polarity drift towards the other electrode. This means that for a diamond detector 500 μm thick the contribution of single carrier type dominates in the induced current, which is monitored by a fast wide-bandwidth amplifier connected to the oscilloscope. A more conventional use of this technique (Transient Current Technique - TCT) employs generation of free carriers by short light pulses. The wide band-gap of diamond would require a fast pulsed laser in the deep ultraviolet region - something that is hardly affordable. More information on the TCT setup used for silicon can be found in Ref. [7]. In order to minimize the effect of trapped charge on space charge, the rate of α-particles was kept at the level of 10 Hz so every pulse was recorded and averaged offline. All the measurements were carried out at room temperature.

3. Single crystalline diamond

The induced current I at the time t after generation of electron-hole pairs in the detector is given by [7]

$$I_{e,h}(t) = \frac{e_0 A N_{e-h}}{W} v_{e,h}(t)\, e^{-t/\tau_{eff,e,h}} \quad , \tag{3.1}$$

where e_0 is the elementary charge, A the amplifier amplification, N_{e-h} the number of generated electron hole pairs, W the detector thickness, $\tau_{eff,e,h}$ the effective trapping times and $v_{e,h}$ the drift velocity of the carriers. The induced currents shown in Fig. 2a,b indicate that the drift velocity is almost constant over the depth at given voltage (i.e. seen as constant induced current after the initial rise), hence the constant electric field exhibiting negligible space charge. High resistivity of the diamond allows for two ohmic contacts and operation is possible at any bias polarity. Therefore the selection between hole and electron signal is simply done by reversing the polarity; positive polarity corresponds to injection of electrons and negative polarity to injection of holes.

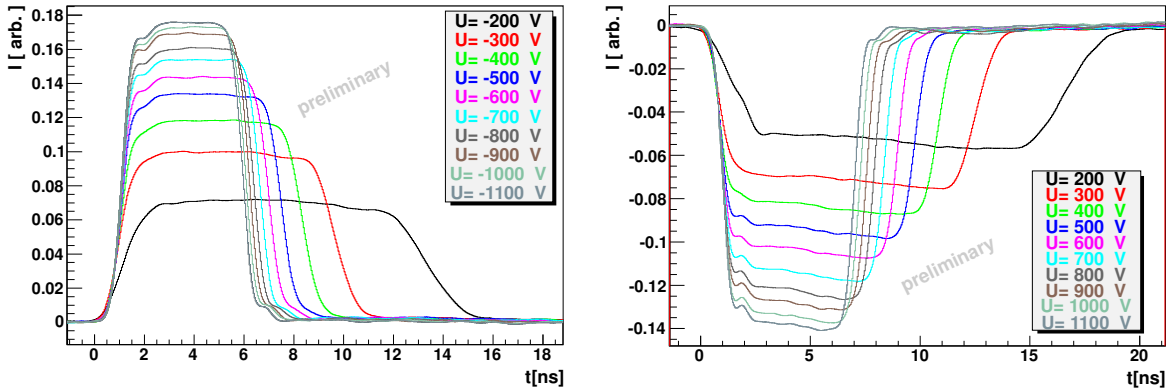

(a) (b)

Figure 2: Induced current signals for (a) hole injection and (b) electron injection in a non-irradiated scCVD detector. The injection was done by exposing detector's back surface to α particles from ^{241}Am source.

A regular procedure used by CERN-RD42 collaboration for priming irradiated detectors is exposure of detectors without bias voltage to a strong source ($\approx$ 37 MBq) of ^{90}Sr electrons for

around a day (> 20 h). The calculated flux of electrons during priming was of the order of few 10^6 cm^{-2} s^{-1}, which corresponds approximately the rate of ionizing particles in an LHC experiment. The induced currents measured in the irradiated scCVD detector to $1.1 \cdot 10^{14}$ cm^{-2} after such priming are shown in Figs. 3 for both electrons and holes. The induced current shape is inclined, which is to a large extent the consequence of trapping term in Eq. 3.1. The other reason could be a non-homogeneous electric field, but in this case the slope for electrons and holes should be different. Therefore it can be assumed that the effective space charge doesn't significantly influence the shape of the induced current.

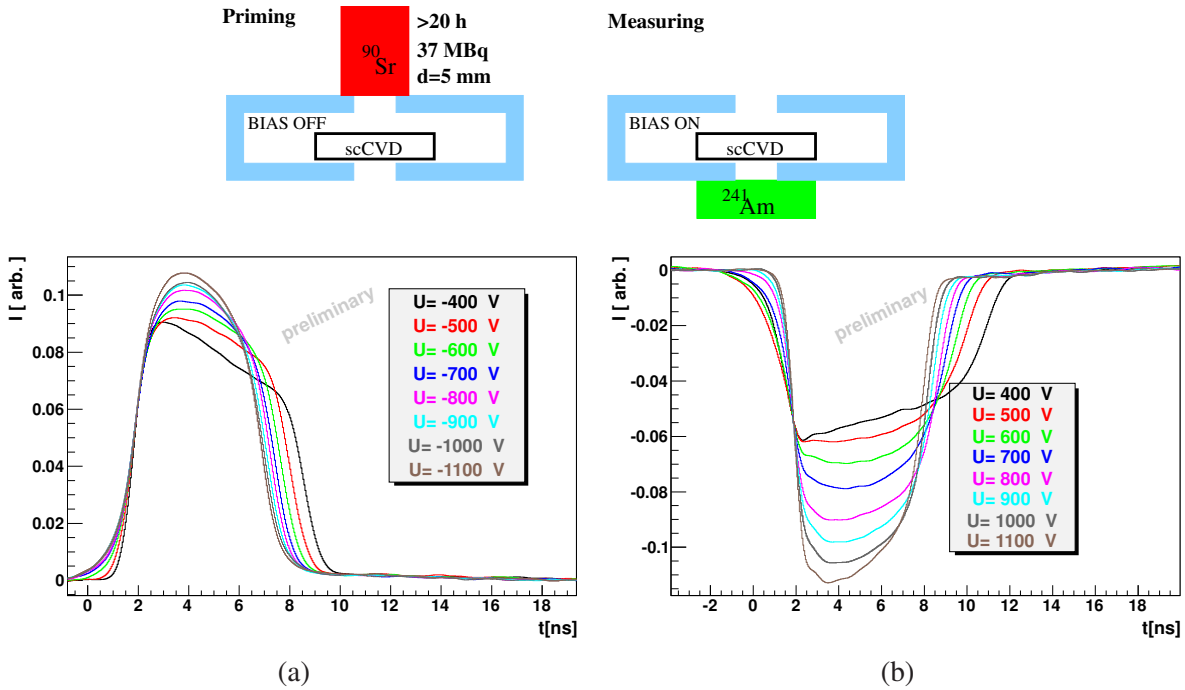

(a) (b)

Figure 3: Induced current signals for (a) hole injection and (b) electron injection in a scCVD detector irradiated to $1.1 \cdot 10^{14}$ fast neutrons/cm^2. The priming was performed without bias. The distance between the source and detector during priming was $d = 5$ mm.

Entirely different induced current pulse shapes as shown in Figs. 3 are obtained if the detector is biased during the priming procedure, as can be seen in Figs. 4. The detector was biased at ± 1 kV and after the priming procedure a voltage scan was performed in the direction from higher to lower voltage. For the electron injection the polarization of the detector causes a strong voltage drop in a narrow region at the injection (back) contact, due to large positive space charge accumulated during priming. The increasing current (i.e. velocity) in time (despite trapping) at lower voltages points to a negative space charge in most of the detector bulk (see curves at 700, 800 and 900 V). In case of hole injection the voltage drop in the region at the injection contact seems to be smaller, but the field in the bulk has a more complex behaviour.

A comparison of the collected (i.e. induced) charge reveals that there is small, if any, difference at the highest voltages between priming with and without bias voltage applied (see Fig. 5). At lower voltages the dependence of collected charge on bias voltage is very strong when detector was primed under bias. Only after bias voltage exceeds 700 V for positive and 400 V for the negative

polarity does the collected charge start to increase. Space charge formed during priming persists also when the voltage is reduced. As the electric field integral between the electrodes should result in applied external voltage, there can be regions in the detector with opposite sign of the electric field (see next section for explanation). The injection of the charge from one side means that the drift ends at the borders of these regions. Hence, the contribution to the collected charge is small. Once the bias voltage is high enough that the whole detector has the same orientation of the field the charge increases rapidly.

On the other hand, if detector is primed unbiased only a moderate rise of the charge with bias voltage can be observed, which is a consequence of faster drift and therefore less trapping. Already after $\approx 10^{14}$ cm^{-2} the trapping of the drifting charge is significant - around 30%, and about equal for both electrons and holes.

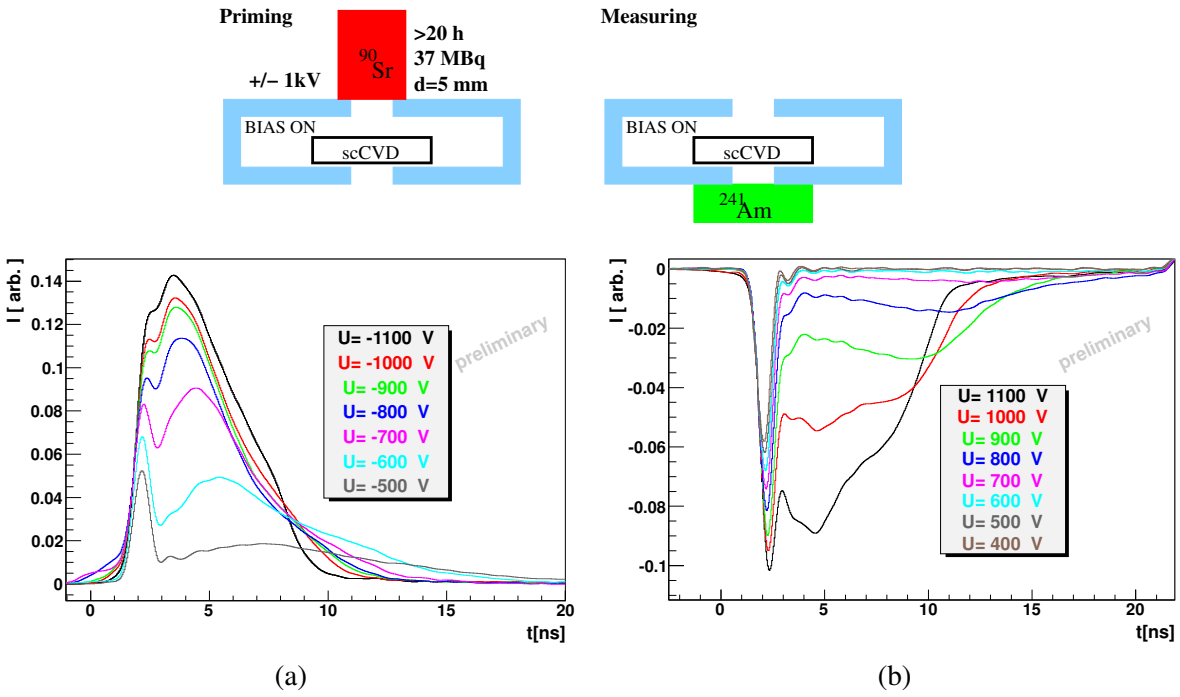

(a) (b)

Figure 4: Induced currents for (a) hole injection and (b) electron injection in a scCVD detector irradiated to $1.1 \cdot 10^{14}$ fast neutrons/cm^2. The priming was performed with bias voltage on.

The transition from the non-polarized detector to steady state polarized detector at ± 1 kV is shown in Fig. 6. After priming without bias voltage the bias was turned on and the induced current from α particles was monitored. The appearance of polarization depends on the particle rate. In order to be able to observe polarization onset on time scale of a day the distance between the priming source (^{90}Sr) and detector was varied/decreased during the measurement. Initially the pulse width for hole signal (Fig. 6a) starts to grow indicating that the electric field in the bulk decreases. The pulses show a double peak profile an indication of high electric field regions at both contacts. However after around 12 h (cyan curve) a steady state is achieved, with narrower pulse widths than those seen after 15 min. A straightforward explanation would be that this is due to the different capture rates of various defects in diamond. The steady state pulses at -1 kV in Fig. 4a and Fig. 6a are in reasonable agreement. Slightly worse agreement was found for electron injection

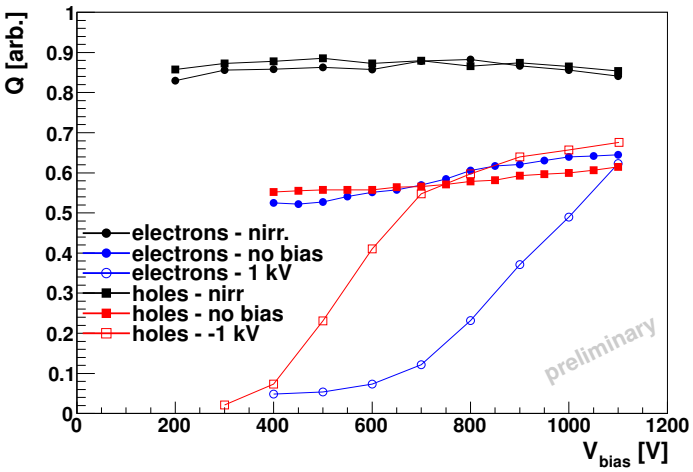

Figure 5: Induced charge (integral of induced current over 20 ns) vs. bias voltage for both priming scenarios; with 1 kV applied and without bias. The induced charge for non-irradiated detector is also shown (black markers).

(see Figs. 4b and 6b).

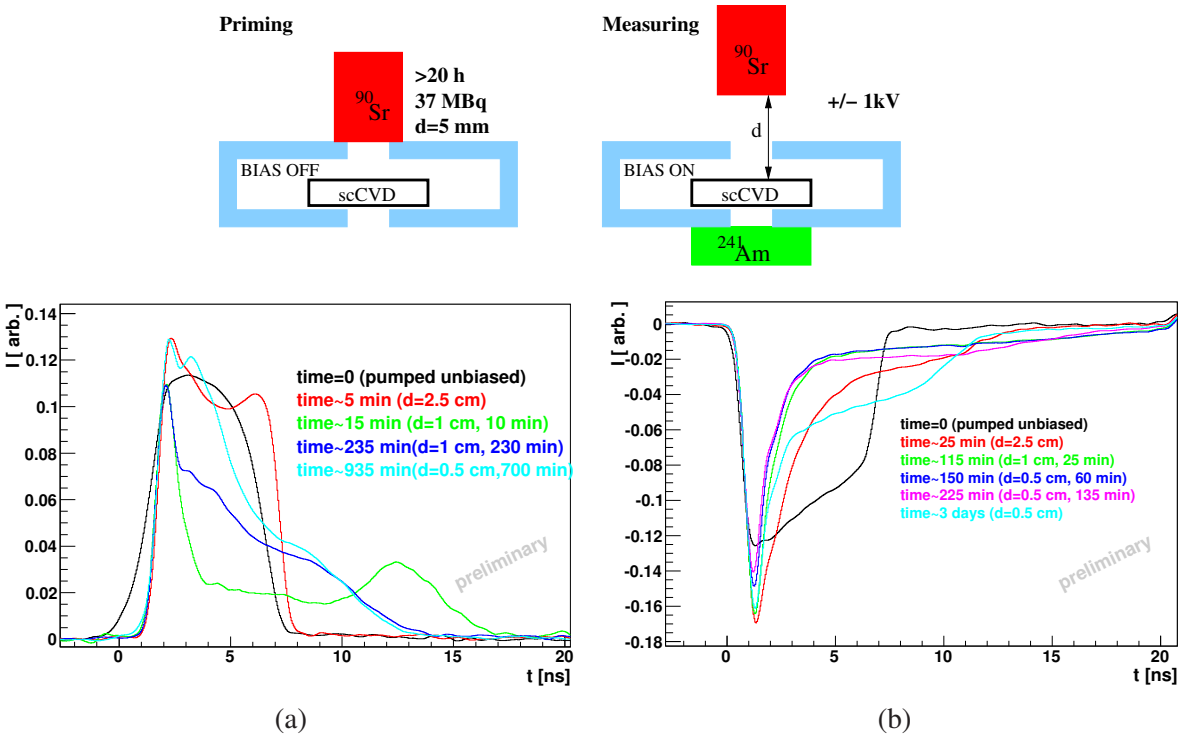

(a) (b)

Figure 6: Induced current signals from the α-source ((a) holes, (b) electrons) during the exposure of detector to different rates of ^{90}Sr electrons after priming with bias off. During the scan the distance between the source and detector was varied. The time spent at given distance is given in the figure legend. The detector bias was 1 kV.

4. Space charge determination for pCVD

Unlike in a scCVD detector the defects are already present in pCVD diamond before irradiation. These defects are probably not homogeneously distributed, but are mainly located at grain boundaries. TCT technique is therefore not very practical as pulses differ regarding to which grain was hit by the alpha particle and the averaging over the many pulses would yield an non-physical picture of the field. Minimum ionizing particles hit many grains over the entire depth of the detector and therefore smear the influence of the impact position on the induced current signal. The generated charge is however too small for a reliable TCT analysis. Instead, we used a integrating amplifier for measuring induced charge in semiconductor detectors (see Fig. 1a).

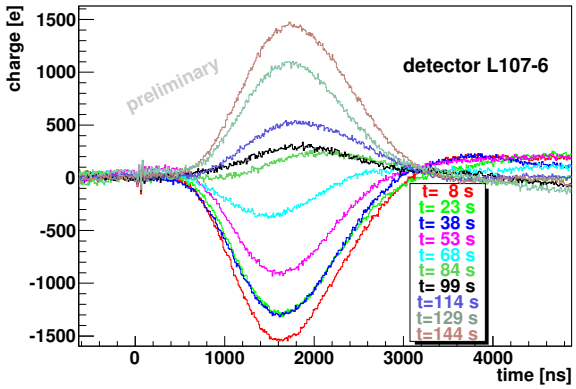

Figure 7: Averaged pulses at the output from a shaping amplifier after changing the bias from -1 kV to -100 V. The colours correspond to time after the bias change. The peak value at the output of the shaping amplifier is proportional to the induced charge after ^{90} Sr electron passage. In steady state at -100 V the signal is around 1900 e.

After priming under bias at $d = 5$ mm for a day, the voltage was promptly changed to a lower value. In Fig. 7 the pulse shapes from a shaping amplifier ($t_{shaping} = 500$ ns) are shown at different times after the bias was changed from -1 kV to -100 V with source at $d = 3$ cm. Immediately after the change the induced charge has negative polarity, which is different than that measured in steady state at -1 kV. It is obvious that after the bias change there are regions in the detector with opposing orientation of the electric field. Moreover, in the larger part of the detector volume the electric field has different orientation than determined by the external bias. The space charge redistributes in time due to trapping/de-trapping processes and approaches the steady state (see. Fig. 7). This is schematically illustrated in Fig. 8. After sudden change of bias the steady state electric field (black line) shifts by $\Delta V_{bias}/W$ retaining the field shape (red dashed line). The induced charge and its sign are in first approximation determined by the difference in widths of the regions with opposing electric field. The redistribution of space charge leads eventually to a new steady state (brown dashed line). Once the latter is reached the direction of the electric field in the entire volume is determined by the external bias.

A set of measurements was performed for different ΔV_{bias}, where *CCD* was measured in the first 8 seconds after the drop of the bias. Prior to the bias change the detector was in steady state at -1 kV. For easier understanding the *CCD* is signed to indicate the polarity of the signal. As can

be seen in Fig. 9a *CCD* changes linearly with ΔV_{bias}. The signal changes sign at $\Delta V_{bias} \sim 720$ V , where the widths of the opposing electric field regions are approximately equal. The space charge concentration N_{eff} can be estimated from $CCD(\Delta V_{bias}, t \sim 0)$ by assuming that the electric field is merely shifted by $\Delta V_{bias}/W$ immediately after the bias change. If *CCD* changes only due to different electric field orientations then the following relation holds:

$$\frac{dE}{dx} \sim \frac{1}{W}\frac{d\Delta V_{bias}}{dCCD} \sim \frac{e_0 N_{eff}}{\varepsilon_c} \quad , \tag{4.1}$$

where ε_C is absolute permittivity of diamond and e_0 the elementary charge. Using the Eq. 4.1 and $dV_{bias}/dCCD$ from the linear fit in Fig. 9a, $N_{eff} \sim 2 \cdot 10^{12}$ cm^{-3} is obtained. It is therefore clear that substantial space charge is present already before irradiation.

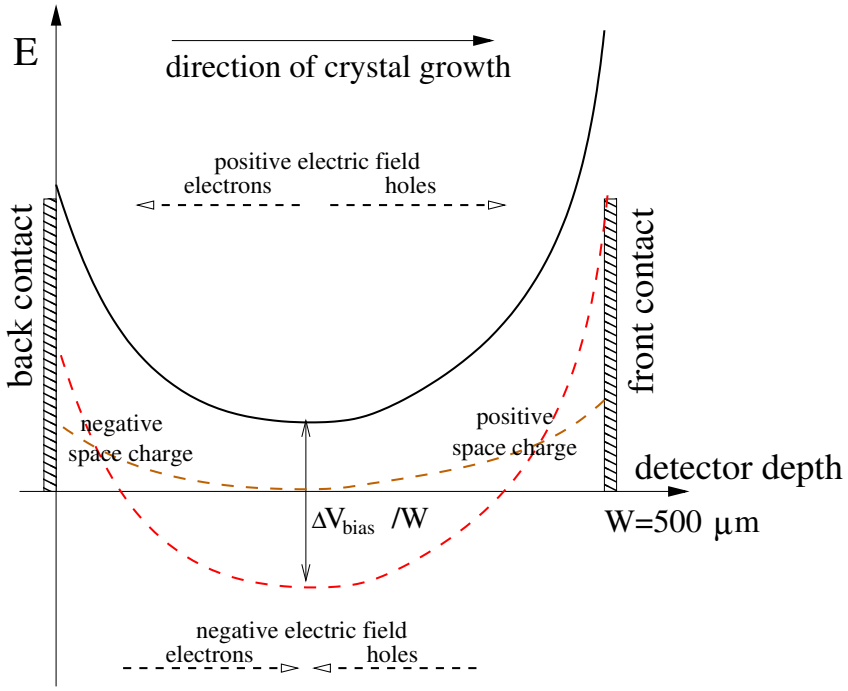

Figure 8: Schematic profile of the electric field in diamond detector: solid black line - steady state operation at -1 kV; dashed red line - immediately after changing the bias by ΔV_{bias}; brown dashed line - the steady state operation at new (lower) bias voltage.

The largest ΔV_{bias} was equal to the maximum bias voltage as the voltage source used did not allow for abrupt change of polarity. After grounding the detector previously biased to ± 1 kV, the evolution of the *CCD* was monitored over more than an hour with source at $d = 3$ cm (see Fig. 9b). Two components can be identified; fast with time constant of few hundred seconds and slow with a time constant of few thousands s. This roughly sets the time scale required for the non-irradiated detector at particle rate given by the source position to reach the steady state. The *CCD* dropped from 250 μm at ± 1 kV to $CCD(t \sim 0) \sim \mp 100$ μm showing that only $\sim 30\%$ of the detector volume retains the electric field orientation of that in the steady state at ± 1 kV. As the integral of the field must vanish that means that electric field strength at both contacts is substantially higher

than in the middle of the detector. This is in an agreement with the field profile of the irradiated scCVD detector investigated by TCT.

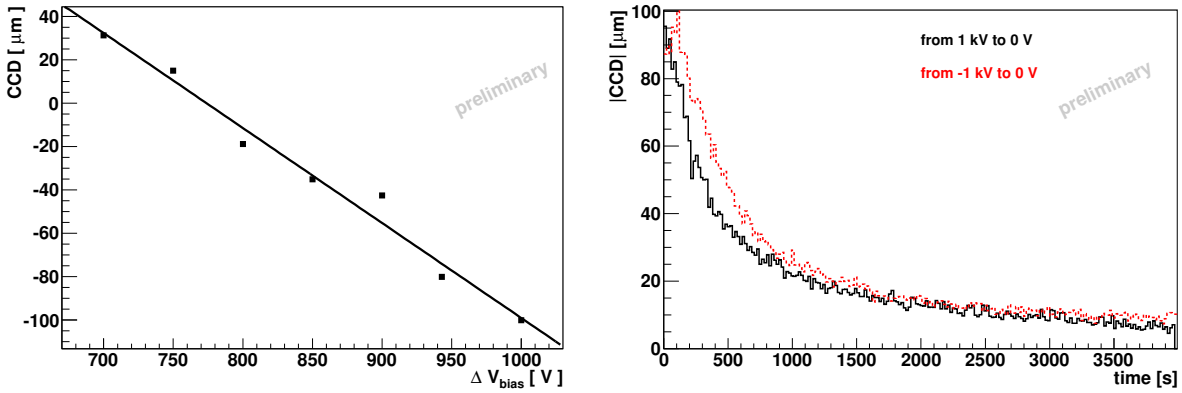

Figure 9: (a) Dependence of *CCD* on the bias voltage drop ΔV_{bias} for a detector biased to -1 kV in steady state. The solid line indicates the linear fit to the measured points. (b) The evolution of $|CCD|$ after the bias was changed from -1 kV to 0 V (black solid) and +1 kV to 0 V (red dashed). The measurements in (a) and (b) were performed with shaping time of 500 ns.

5. Conclusions

The polarization of diamond detectors was investigated with irradiated scCVD detector and also with non-irradiated pCVD detector. It has been shown that the electric field in the diamond detector depends strongly on bias voltage and particle rate. Therefore the priming procedure should always be carried out at conditions close to that of the real application in order to obtain relevant results. A new method was proposed to estimate space charge and rough shape of the electric field in pCVD diamond detectors, where a conventional Transient Current Technique is difficult to apply. It has been shown that even a non-irradiated detector is polarized with a space charge in the range of few 10^{12} cm^{-3}.

References

[1] F. Gianotti et al., hep-ph/0204087, 2002.

[2] R. S. Sussmann, CVD Diamond for Electronic Devices and Sensors, Wiley, 2009 ,ISBN: 978-0-470-74036-1.

[3] H. Kagan et al.,"RD42 Status Report: Development of Diamond Tracking Detectors for High Luminosity Experiments at the LHC", CERN-LHCC-2008-005, 2008.

[4] S. Zhao, "Characterization of the Electrical Properties of Polycrystalline Diamond Films", Ph.D. Dissertation, Ohio State University (1994).

[5] L. Snoj et al., Appl. Radiat. Isot. 70 (2012) p. 483.

[6] G. Kramberger et al., Nucl. Instr. and Meth. A 554 (2005) p. 212.

[7] G. Kramberger et al., Nucl. Instr. and Meth. A 476 (2002) p. 645.